Texture Classification Algorithm Using RGB Characteristics of Soil Images

Chung, Sun-Ok
Department of Biosystems Machinery Engineering, Collage of Agricultural and Life Sciences, Chungnam National University

Cho, Ki-Hyun
Department of Crop Science, Collage of Agricultural and Life Sciences, Chungnam National University | Department of Biosystems Machinery Engineering, Collage of Agricultural and Life Sciences, Chungnam National University

Cho, Jin-Woong
Department of Crop Science, Collage of Agricultural and Life Sciences, Chungnam National University | artment of Crop Science, Collage of Agricultural and Life Sciences, Chungnam National University

Jung, Ki-Youl
National Academy of Crop Science

他

https://doi.org/10.5109/25196

出版情報：九州大学大学院農学研究院紀要. 57 (2), pp.393-397, 2012-09-20. Faculty of Agriculture, Kyushu University
バージョン：
権利関係：

J. Fac. Agr., Kyushu Univ., **57** (2), 393–397 (2012)

Soil Texture Classification Algorithm Using RGB Characteristics of Soil Images

Sun–Ok CHUNG[1], Ki–Hyun CHO[1], Jin–Woong CHO[2]*, Ki–Youl JUNG[3] and Takeo YAMAKAWA

Laboratory of Plant Nutrition, Division of Molecular Biosciences, Department of Biosciences & Biotechnology, Faculty of Agriculture, Kyushu University, 6–10–1 Hakozaki, Fukuoka 812–8581, Japan

(*Received April 24, 2012 and accepted May 10, 2012*)

Soil texture has an important influence on agriculture, affecting crop selection, movement of nutrients and water, soil electrical conductivity and crop growth. Soil texture has traditionally been determined in the laboratory using pipette and hydrometer methods that require a considerable amount of time, labor, and expense. Recently, in–situ soil texture classification systems using optical diffuse reflectometry or mechanical resistance have been reported, especially for precision agriculture where more data is needed than in conventional agriculture. This paper is a part of overall research to develop a soil texture classification system using image processing. Application of image processing was motivated by simple traditional approaches such as visual inspection and the "hand–feel" method. In this paper, the potential of soil texture classification using RGB histograms was investigated. Seven sites representing major Korean paddy soil series were selected, 4–6 core samples up to a 50–cm intervals. For each segmented soil sample, four surface images were taken using a miniaturized CCD camera, and texture fractions were determined by the pipette method. Scatter plots showed linear patterns between silt content and histogram variables such as brightness (averaged pixel value), skewness, and difference between mode value and brightness ("mode–brightness"). When 5%–averaged silt content was linearly regressed with "mode–brightness", squared correlation coefficient (R^2), root mean square error of calibration (RMSEC), and root mean squared error of prediction (RMSEP) were 0.96, 2.2%, and 6.3%, respectively. When soils were classified using USDA soil texture classification, the laboratory method and the in–situ image processing method produced the same results for 48% of the samples.

Keywords: image processing, precision agriculture, RGB histogram, soil sensor, soil texture

INTRODUCTION

Precision agriculture requires acquisition and management of data on soil and crop properties. In particular, soil properties significantly affect crop selection and growth management (Bae *et al*., 2004). Among soil properties, soil texture is a main property not only related to other soil properties such as soil electrical conductivity, water and nutrient content, but also affecting management practices such as tillage, fertilizer and pesticide application (Hur, 1993; Lee *et al*., 2005). Therefore, quantification of soil texture is very important for successful field and crop growth management.

Conventionally, soil texture indicates sand, silt, and clay fractions within soil based on USDA criteria, and has been laboratory–determined using pipette and hydrometer methods, which are labor–, time–, and cost–consuming (Gee and Or, 2002). Therefore, *in–situ* rapid methods are more preferable for precision agriculture than these laboratory methods. Mechanical, optical, and electrical approaches have been reported for *in–situ* rapid determination of soil texture. Douglas and Olsen (1981) suggested using cone penetrometer data for soil classification. Zuo *et al*. (2000) used a fiber–optic sensor moving at a speed of 5.08 mm/s and sampling at rates of 10, 100, and 200 Hz. Starr *et al*. (2000) applied a dielectric method relating soil texture fractions to changes in electrical dipole moments. These methods measure optical reflectance, mechanical resistance, or electrical properties of soil and then relate them to texture fractions.

It is known that soil survey experts evaluate soil texture *in–situ* using visual inspection and the "hand–feel" methods based on many years of experience. They visually examine color and size of aggregated soil particles, and feel roughness by fingers. Our approach using image processing was motivated by this visual inspection and "hand–feel" method, taking surface imagery of soil samples, and calculating size distribution or roughness of soil particles. Image processing has been used in a variety of agricultural applications such as estimation of properties related to not only soil and crop, but also quality of agricultural products for sorting and grading (e.g., fruits) (Lim, 2003; Breul and Gourves, 2006). Lieberman *et al*. (2000) patented an *in situ* microscope imaging system for examining subsurface environments fabricated in a soil penetrating tube, but have not used the system for soil classification.

Soils with different sand, silt, and clay fractions may have different colors due to interactions with other soil properties (e.g., oxidation and reduction), and different types and amounts of rock–forming minerals (Breul and Gourves, 2006), and these characteristics could be used for soil classification variables. As a part of overall

[1] Department of Biosystems Machinery Engineering, Collage of Agricultural and Life Sciences, Chungnam National University, Daejeon, Korea
[2] Department of Crop Science, Collage of Agricultural and Life Sciences, Chungnam National University, Daejeon, Korea
[3] National Academy of Crop Science, Milyang, Korea
* Corresponding author (E–mail: jwcho@cnu.ac.kr)

research to develop a soil classification system using image processing, the objective of the paper was to develop a soil texture classification algorithm using RGB characteristics of soil images such as averaged pixel value (brightness) and skewness.

MATERIALS AND METHODS

Soil sampling and texture analysis

To develop a soil texture classification algorithm, 194 soil samples from 7 selected Korean paddy fields were used. Sampling sites were selected considering dominant soil series with different texture fractions of paddy fields, with related information given in Table 1. From each site, 6 to 7 soil cores (diameter: 50–mm) were obtained using a core sampler up to 30 to 50 cm depths, depending on field conditions, and segmented by 50–mm intervals (Fig. 1). For each segmented sample, 4 images (2 from each side) were taken. After image acquisition, sand, silt, and clay fractions of the samples were determined using the sieve–pipette method (Gee and Or, 2002). Table 1 summarizes soil series and texture fractions of the samples.

Image acquisition and processing

Our goal was to develop a portable *in–situ* soil texture classification system using image processing. Two alternative platforms were considered: a moving platform that took soil surface imagery traveling through the soil profile by incorporation of the sensor in another sensing system (e.g., cone penetrometer), or a stationary platform that captured surface imagery of soils obtained by a soil sampler (e.g., auger). Therefore, the image acquisition sensor for *in–situ* soil texture classification system needed to be smaller and lighter. After market survey, a magnification–controllable CMOS image sensor (Model: USB 2.0 PC camera SN9C201, Sonix Inc., Springfield, Virginia, USA) was selected for our study. Diameter and height of the camera were 3 cm and 9 cm, respectively. Magnification up to 22.25 was controlled by rotating the front lens and the ratio was calculated and confirmed by comparing pixel numbers of the reference and sample images. The camera obtained images of size 640 × 480 pixels, and stored RGB values in 8 bits (256 levels). Soil samples were located in a small box with an illumination intensity of about 115 Lux controlled by white LEDs.

Fig. 2 shows examples of soil surface images and corresponding histograms of gray level pixel values (i.e., brightness). Images of soil samples with different texture fractions contained quite different features (e.g., crevice; circled areas in Fig. 2) and quality (e.g., roughness, brightness). Overall, as sand fractions increased, numbers of brighter pixels increased. For example, an image of soil with high sand fraction showed greater pixel values than an image with high silt and clay fractions (Fig. 2). Therefore, we expected that shape of the histograms (e.g., central tendency, dispersion, or bias) would be related to soil textural fractions.

As variables representing shape of these pixel value

Fig. 1. Photos of soil core sampling (left) and surface image of the sample (right).

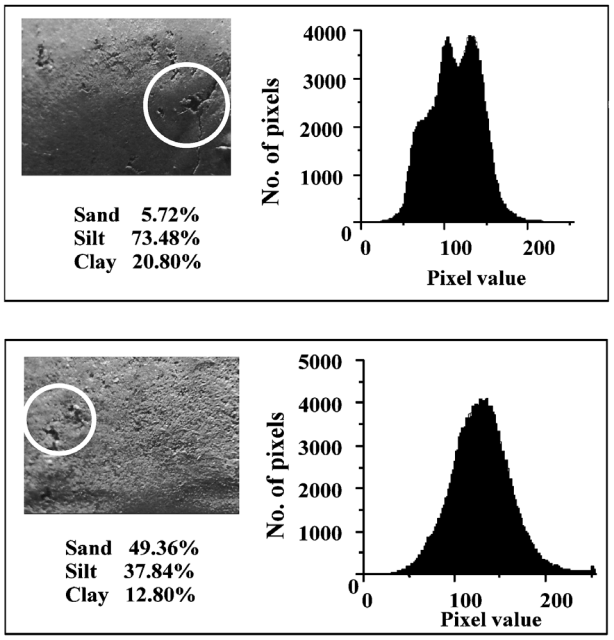

Fig. 2. Example images and gray level brightness histogram for soils with high silt fraction (top) and sand fraction (bottom).

Table 1. Specifications of the soil samples

Site	Series	Sand (%)		Silt (%)		Clay (%)		No. of Sample
		Mean	STD	Mean	STD	Mean	STD	
1	Hwadong	9.4	1.5	58.5	1.7	32.1	1.2	30
2	Gyuam	11.7	2.3	6.8	3.1	20.5	2.2	30
3	Gangseo	38.3	3.6	46.9	3.4	14.9	1.4	28
4	Pyeongtaeg	11.2	2.0	55.0	5.1	33.8	4.6	36
5	Honam	15.9	6.9	48.1	6.4	36.0	4.2	22
6	Yungnam	13.9	5.2	58.2	5.6	27.9	2.7	23
7	Pyeongtaeg	20.0	8.3	39.4	14.9	40.6	11.0	25

histograms, we chose averaged pixel value (brightness), difference between median value and brightness ("median –brightness"), difference between mode value and brightness ("mode–brightness"), and skewness. Procedures to investigate relationships between laboratory–determined soil texture fractions and these histograms parameters were: 1) vacant pixels or areas (e.g., crevice) were blanked, 2) RGB pixel values were combined to gray level pixel values, and histogram variables were calculated, and 3) each of the histogram variables and texture fractions (i.e., sand, silt, and clay %) were linearly regressed. This procedure was implemented using MatLAB software (The MathWorks, Inc., Natick, MA, USA). Half of the samples were used for development of regression models and the other half were used for validation of the models to reduce possibility of over–fitting.

RESULTS AND DISCUSSION

Fig. 3 shows example scatter plots between histogram variables and soil texture fractions. Silt content showed the clearest linear pattern for all of the histogram variables, and correlation coefficients were negative for brightness and skewness, and positive for "median–brightness" and "mode–brightness".

Clay content showed somewhat opposite patterns to silt content with the histogram variables, but the patterns were less clear compared with silt content. Sand content did not show any linear patterns with the histogram variables. These relationships led to the conclusion that, overall, soils with greater amount of silt content resulted in darker soil images and soils with greater amount of clay content resulted in brighter soil images.

Table 2 summarizes linear regression between soil texture fractions (Y) and gray level histogram variables

Table 2. Results of linear regressions between soil texture fractions (Y) and histogram variables of the sample images (X)

Y (%)	Y processing*	X	Regression results		
			R^2	RMSEC (%)	RMSEP (%)
Sand	Y	Mode – brightness	0.05	10.2	10.4
	$\sqrt[4]{Y}$	Mode – brightness	0.06	0.3	0.3
	Y_{out}	Brightness	0.10	10.1	10.3
	$Y_{5\%}$	Skewness	0.35	10.3	12.1
Silt	Y	Mode – brightness	0.20	10.7	9.2
	$\sqrt[4]{Y}$	Mode – brightness	0.18	0.2	0.1
	Y_{out}	Brightness	0.30	7.0	7.9
	$Y_{5\%}$	Mode – brightness	0.96	2.2	6.3
Clay	Y	Mode – brightness	0.08	10.1	8.4
	$\sqrt[4]{Y}$	Mode – brightness	0.07	0.2	0.2
	Y_{out}	Mode – brightness	0.05	8.9	7.2
	$Y_{5\%}$	Mode – brightness	0.17	10.8	8.4

*Y_{out}: outlier removed Y, $Y_{5\%}$: 5%-averaged Y

Table 3. Comparison of soil classification using the laboratory method with that using image processing method

Site	Laboratory method		Image processing method	
	Classified texture	No. of sample	Classified texture	No. of Sample
1	Silt clay loam	15	Silty clay loam	15
2	Silt loam	15	Silty clay loam Clay loam	14 1
3	Loam	14	Silty clay loam Clay loam	13 1
4	Silt clay loam	18	Silty clay loam	18
5	Silt clay loam Clay loam	9 2	Silty clay loam Clay loam	5 6
6	Silt clay loam Silt loam	3 9	Silty clay loam	12
7	Silt clay loam Silt clay Clay loam Clay Loam	4 4 2 1 1	Silty clay loam	12

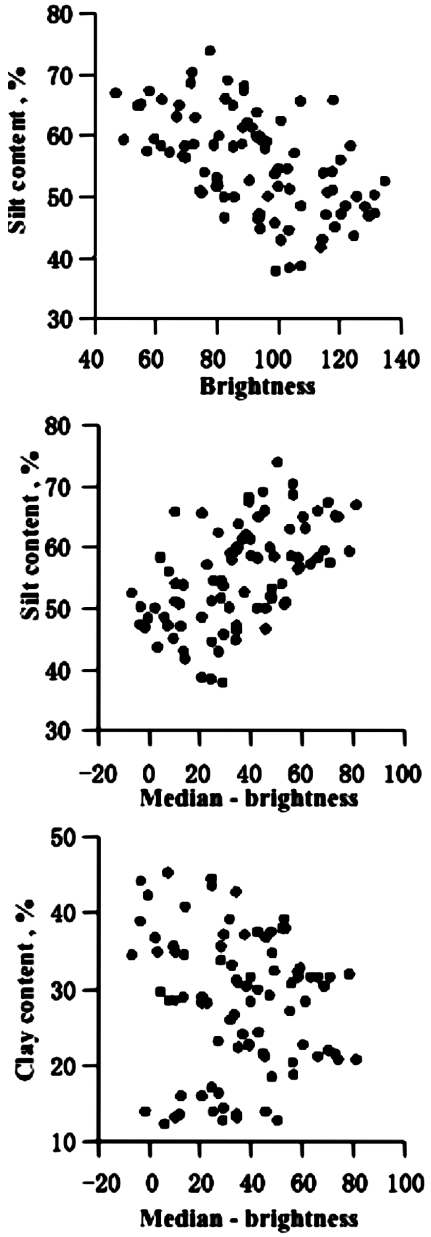

Fig. 3. Example scatter plots between histogram variables and soil texture fractions.

of the sample images (X). X variables producing the highest coefficients of determination were reported. Generally coefficients of determination of the calibration models were quite low (less than 0.20) and RMSEC values were greater than 10% for all of the texture fractions. The best model was obtained for silt (R^2=0.20; RMSEC=10.7%) with "mode–brightness" as the X variable.

In many cases, Y variables had quite large variances and the variances were not equal, therefore several transformations of Y were tried to improve regression performance: power, logarithmic, and exponential transformations. The most improved regression models were obtained when a power of 1/4 was applied to Y.

Some soil images presented problematic areas, for example, containing a large portion of cracks and crevices, therefore images of 10 samples were removed as outliers. Removing 10 data points out of 194 in the original data set (Y_{out}) improved regression performance in many cases. For example, R^2 increased from 0.05 to 0.10 for sand content and from 0.20 to 0.30 for silt content.

Errors in pixel values of soil surface images and laboratory–determined soil texture fractions might be induced by soil sampling, laboratory determination, and image acquisition processes. These errors could be overcome by increasing the number of measurements or averaging the measurements. When soil texture measurements were averaged with intervals of 1, 3, 5, and 7% fractions, R^2 values for silt content changed to 0.27, 0.46, 0.96, and 0.96. For 5%–averaged texture fractions, R^2 values obtained using linear models for sand and clay contents were 0.35 and 0.17, respectively.

Using a validation data set, soil classification by USDA soil texture classification using the laboratory method was compared with that using the image processing method. As summarized in table 3, about 48% of the samples were classified into the same soil texture, and some of the other samples produced similar soil texture classification.

In this paper, we tried several different ways to classify soil texture using processing of soil surface images taken in field conditions. Both laboratory determined soil texture and soil surface images might be erroneous due to soil sampling, laboratory analysis, or image acquisition procedures. Although clear linear relationships between the two data sets were not found, some potential of *in–situ* soil classification was observed, especially for silt content.

Variables from gray level (averaged RGB pixel value) histograms were investigated in this paper. Using all histograms for R, G, and B values might provide better relationships with soil texture fractions since different optical bands might be associated with different reflectance characteristics caused by different texture fractions in the samples. Different variable transformations and averaging could be applied. Some other approaches such as Fourier transformation to investigate frequency domain aspects, and application of artificial intelligence techniques might be also useful. These issues will be investigated in future research.

ACKNOWLEDGMENTS

This work was supported by the Korean Research Foundation Grant funded by the Korean Government (MOEHRD) (KRF–2007–331–D00605).

REFERENCES

Bae, S. G., I. K. Yeon, S. D. Park, C. K. Kang, C. K and K. Zakaullah 2004 Effects of soil texture by soil addition on the growth and quality of oriental melon (*Cucumis melo* L. var. makuwa Mak.) under protected cultivation. *J Bio–Environ. Con.*, **13**(3): 156–161

Breul, P. and R. Gourves 2006 In field soil characterization: approach based on texture image analysis. *J Geotech. Geoenviron. Eng.*, **132**(1): 102–107

Douglas, B. J. and R. S. Olsen 1981 Soil classification using electric cone penetrometer. *In* "Cone Penetrometer Testing and

Experience", ed. by G. M. Norris and R. D. Holtz, American Society of Civil Engineers, New York, pp. 209–227

Gee, G. W. and D. Or 2002 Particle–size analysis. *In* "Methods of Soil Analysis: Part 4. Physical Methods", ed. by J. H. Dane and G. C. Topp, SSSA, Madison, Wisconson, pp. 255–293

Hur, B. K. 1993 Effect of tillage methods on rice yield and soil properties under different soil textures. *Korean J. Crop Sci*., **38**(3): 290–295

Lee, S. M., S. S. Kim, D. S. Park and J. H. Hur 2005 Mobility of pesticides in different soil textures and gravel contents under soil column. *Korean J. Pesticide Sci*., **9**(4): 330–337

Lieberman, S. H., D. S. Knowles and L. J. Martini 2000 In situ microscope imaging system for examining subsurface environments. US patent number: 6, 115, 061

Lim, D. H. 2003 Development of a fruit sorting system using statistical image processing. *Korean J. App. Statistics*, **16**(1): 129–140

Starr, G. C., P. Barak, B. Lowery and M. Avila–segura 2000 Soil particle concentrations and size analysis using a dielectric method. *Soil Sci. Soc. Am. J*., **64**: 858–866

Zuo, Y., D. C. Erbach and S. J. Marley 2000 Soil structure evaluation by using a fiber–optic sensor. *Trans. ASAE*, **43**(6): 1317–1322